DEVELOPMENTAL DYNAMICS 226:540–550, 2003

ARTICLE

Cardiac Neural Crest in Zebrafish Embryos Contributes to Myocardial Cell Lineage and Early Heart Function

Yin-Xiong Li,[1] Marzena Zdanowicz,[1] Lori Young,[2] Donna Kumiski,[2] Linda Leatherbury,[2,3] and Margaret L. Kirby[1]*

Myocardial dysfunction is evident within hours after ablation of the cardiac neural crest in chick embryos, suggesting a role for neural crest in myocardial maturation that is separate from its role in outflow septation. This role could be conserved in an animal that does not have a divided systemic and pulmonary circulation, such as zebrafish. To test this hypothesis, we used cell marking to identify the axial level of neural crest that migrates to the heart in zebrafish embryos. Unlike the chick and mouse, the zebrafish cardiac neural crest does not originate from the axial level of the somites. The region of neural crest cranial to somite 1 was found to contribute cells to the heart. Cells from the cardiac neural crest migrated to the myocardial wall of the heart tube, where some of them expressed a myocardial phenotype. Laser ablation of the cardiac premigratory neural crest at the three- to four-somite stage resulted in loss of the neural crest cells migrating to the heart as shown by the absence of AP2- and HNK1-expressing cells and failure of the heart tube to undergo looping. Myocardial function was assessed 24 hr after the cardiac neural crest ablation in a subpopulation of embryos with normal heart rate. Decreased stroke volume, ejection fraction, and cardiac output were observed, indicating a more severe functional deficit in cardiac neural crest-ablated zebrafish embryos compared with neural crest–ablated chick embryos. These results suggest a new role for cardiac neural crest cells in vertebrate cardiac development and are the first report of a myocardial cell lineage for neural crest derivatives. ***Developmental Dynamics 226:540–550, 2003.*** **© 2003 Wiley-Liss, Inc.**

Key words: zebrafish; heart development; cardiac neural crest; ablations; ventricular function

Received 19 August 2002; Accepted 22 November 2002

INTRODUCTION

In the chick cardiac neural crest ablation model, a distinctive pattern of malformations and myocardial dysfunction develops (Kirby and Creazzo, 1995). The malformations include persistent truncus arteriosus and abnormal repatterning of the bilaterally symmetrical aortic arch arteries to the great arteries (Bockman et al., 1987, 1989). The earliest indication of abnormal development is a primary alteration in myocardial function that appears as early as stage 14. This timing is long before the cardiac neural crest cells would have any contact with the myocardium in an intact embryo (Waldo et al., 1996, 1998). The earliest myocardial functional abnormalities are (1) reduced ejection fraction, (2) decreased calcium current, and (3) abnormal excitation–contraction coupling (Leatherbury et al., 1991; Creazzo, 1990; Creazzo et al., 1997). The same myocardial functional deficit is observed in mouse embryos with deficient neural crest migration (Conway et al., 1997). During this period in normal development, neural crest cells populate the caudal pharyngeal arches and interact with endothelial cells of the

[1]Neonatal-Perinatal Research Institute, Division of Neonatology, Department of Pediatrics, Duke University Medical Center, Durham, North Carolina
[2]Developmental Biology Program, Institute of Molecular Medicine and Genetics, Medical College of Georgia, Augusta, Georgia
[3]Department of Cardiology, Children's National Medical Center, Washington, D.C.
Grant sponsor: National Institutes of Health; Grant number: HL36059; Grant number: HD17063; Grant number: HD39946.
*Correspondence to: Margaret L. Kirby, 307B Nanaline, Research Drive, Duke University Medical Center, Durham, NC 27712.
E-mail: mlkirby@duke.edu

DOI 10.1002/dvdy.10264

aortic arch arteries, endodermal, and ectodermal cells of the ventral pharynx (Waldo et al., 1996). Almost 48 hr elapse before neural crest cells migrate into the outflow tract (Waldo et al., 1998, 1999).

Recent studies in chick have indicated that myocardial dysfunction caused by cardiac neural crest ablation can be averted by exposure of the myocardium to FGF8 blocking antibody (Farrell et al., 2001). FGF8 is expressed in the ventrolateral pharynx by both endodermal and ectodermal cells, which are the first cells contacted as the cardiac neural crest cells initially migrate into the caudal pharyngeal arches (Waldo et al., 1996). Because myocardial dysfunction occurs long before neural crest cells migrate into the cardiac outflow tract where they participate in outflow septation, it is thought to be completely independent from septation events. If this is the case, then the role that neural crest cells play in myocardial maturation may be conserved across a wide range of vertebrate species, including those with little or no outflow tract septation.

The zebrafish has a completely undivided, although complicated outflow tract and appears to be a good model system to investigate a potential role of neural crest cells in myocardial maturation. Morphologically and physiologically, cardiovascular development in the zebrafish is similar to that of mammals and avians (Fishman and Chien, 1997; Hu et al., 2000). A segmental series of branchial arches is formed by neural crest and paraxial mesoderm migration during the first 72 hours postfertilization (hpf; Schilling and Kimmel, 1994; Kimmel et al., 1995). Labeling of premigratory neural crest cells at the branchial arch level results in clonal progeny that are confined to single branchial segments and, generally, single cell types (Schilling and Kimmel, 1994), suggesting that arch precursors may be specified as to fate before formation of the arches. The cranial arches are set aside for development of structures related to the jaw, whereas the caudal arches support development of the aortic arch arteries that will be remodeled into gill arteries (Goodrich, 1958). At 48 hpf, the zebrafish heart consists of a smooth-walled tube partitioned into four segments identifiable by external constrictions between the segments. The myocardium is one-cell thick except in the ventricle, which has two to three cell layers (Hu et al., 2000).

Because cardiac neural crest has not been specifically described in the zebrafish embryo, we undertook to identify cardiac neural crest cell populations that migrate to the heart and map their origin. We found that the zebrafish cardiac neural crest originates from a more rostral axial level than the cardiac neural crest in chick and mouse embryos. Cardiac neural crest cells that migrate to the heart were found in the myocardial wall, and some of them expressed myosin heavy chain, suggesting that they adopted a cardiomyocyte cell lineage. Ablation of the premigratory cardiac neural crest cells was done by using laser irradiation, which eliminated neural crest cell migration to the heart. In the absence of cardiac neural crest, zebrafish cardiogenesis was affected morphologically and functionally in that a significant portion of embryos failed to undergo heart looping and all parameters of ventricular function were depressed in a population of embryos with normal heart rate.

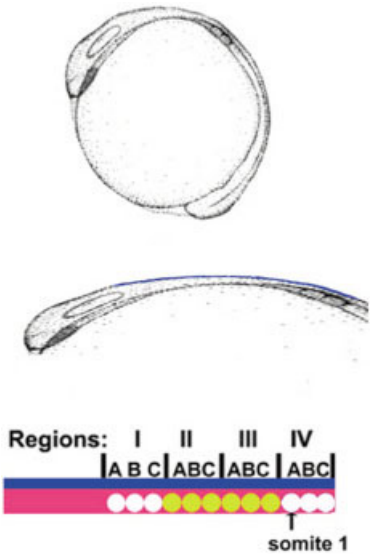

Fig. 1. Diagrammatic representation of the regions of neural crest that were traced to find the axial origin of the cardiac neural crest. The top panel shows a stylized zebrafish embryo as it develops on the yolk at 10.5–11 hours postfertilization. The developing eye is located in the cranial end of the embryo (to the left). In the middle panel, the embryo has been removed from the yolk and flattened. Premigratory neural crest is shown by the blue line. Three somites can be seen. In the bottom panel, the neural crest has been divided into four regions that are each the length of three somites. Region IV actually encompasses somites 1–3. The cardiac neural crest, indicated by yellow circles, was found to arise primarily from regions II and III.

RESULTS

Presomitic Neural Crest Cells Migrate to the Zebrafish Heart

For neural crest cell fate mapping, the cranial neural tube was divided into four regions (Fig. 1): region I was designated as the most cranial axial level with neural crest derivatives; regions II, III, and IV were located successively more caudally such that region IV coincided with somites 1–3. Each region was approximately equivalent to three somite lengths designated subregions A, B, and C. For cell fate mapping, fluorescein was uncaged in premigratory neural crest cells in each region (Stainier and Fishman, 1993, 1994). The number of embryos examined for each region are shown in Table 1A. Two examples of labeled premigratory neural crest populations in the dorsal neural tube are shown in Figure 2 within minutes of the uncaging.

The results of the survey of regions are shown in whole-mounts in Figure 3, although the descriptions presented below were confirmed in frozen sections of all the embryos (data not shown). We found it essential to verify the data histologically to assess the number of labeled cells that migrated to the heart. When fluorescein was uncaged in the dorsal neural tube in region I, neural crest cells were found to migrate primarily to the region of the developing eye (Fig. 3A,E,I). Neural crest cells emanating from the rostral portion of region II mostly migrated to the jaw, although a few cells were found in the heart. Cells emanating from the caudal portion of region II migrated mostly to the region of the cardiac outflow tract (Fig. 3B,F,J). Neural crest cells emanating from the ros-

tral portion of region III migrated mostly to the region of the ventricle and atrium. A few cells in the caudal portion of region III migrated to the heart (Fig. 3C,G,K). Cells from all of region IV (corresponding to somites 1–3) migrated to the trunk caudal to the heart, although 3 of 121 embryos examined showed at least one labeled cell in the heart (Fig. 3D,H,L). In summary, the majority of neural crest cells migrating to the heart were found to originate from regions II and III (Table 1A). Both of these regions are cranial to somite 1. It was unexpected that uncaging fluorescein in premigratory neural crest cells at the level of somites 1–3 yielded no fluorescent cells that could be visualized grossly in the zebrafish heart (Fig. 3). The labeled cells migrated essentially ventrally with very little deviation cranially or caudally from the axial level of somites 1–3 (Fig. 3). In the zebrafish, the heart is located on the yolk almost directly under the head, whereas somite 1 is located approximately one third of the length of the craniocaudal axis. If neural crest cells migrated from the level of somites 1–3 to the heart, they would be required to migrate almost directly cranially. Although this route is certainly possible, we saw no evidence of cranially migrating cells from the somite axial levels. This finding indicates that there is not a perfect match in the neural crest map between chick and zebrafish embryos.

TABLE 1A. Number of Embryos Observed After Dye Uncaging

Dye uncaged in region	Number of embryos	Embryos with labeling in heart	%
I	138	5	3.6
II	151	106	70.2
III	166	126	75.9
IV	121	3	2.5

TABLE 1B. Number of Embryos Analyzed to Confirm Neural Crest Ablation or Heart Phenotype

Procedure	Number of embryos	Confirmed embryos with neural crest–ablation or heart phenotype	%
AP2 in situ hybridization	26	18	69
HNK1 immunohistochemistry	23	12	52
Failure of heart looping	63	13	20.6
Depressed heart rate	39	7	17.9

Myocardial Cell Lineage of Zebrafish Cardiac Neural Crest

For cell lineage analysis, smaller regions of neural crest cells in the caudal portion of region II (BC) were labeled by dye uncaging and the cells followed into the heart. These embryos were sectioned transversely and stained immunohistochemically with MF20, a myocardial marker, to confirm that the fluorescein-positive neural crest cells were localized in or near the heart. The fluorescein-positive cells colocalized with the MF20-positive myocardium of the outflow tract (Fig. 4) and were themselves MF20-positive, indicating that they expressed myosin heavy chain.

Subregions A and B of region III were examined in the same manner. The cells from these subregions were found intermingled with ventricular myocardium and were also MF20-positive (data not shown). A significant population could be seen in the dorsal mesocardium connecting the ventricle with the body wall. The dorsal mesocardium was also MF20-positive (data not shown).

Next, we examined the proportion of neural crest-derived myocardial cells from regions II and III that contributed to specific segments of the cardiac loop (Fig. 5) (Table 2). Region II was found to contribute most cells to the ventricle and outflow myocardium, whereas region III contributed most cells to the inflow and atrial myocardium, although there was a mild degree of overlap (Fig. 5) (Table 2). Eighteen to 23% of the myocardial cells in the outflow tract and ventricle were derived from neural crest originating in region II. Region III contributed 25% of the myocardium to the atrium and 12% to the inflow (Table 2).

Because of the potential for stem cells to form hybrid cells with myocardial cells (Terada et al., 2002), we used high-resolution confocal imaging to determine whether MF20-positive neural crest cells were binucleated. We found no instances of hybrid cells in this population. These results suggest that cardiac neural crest cells in zebrafish are incorporated into the wall of the developing heart as myocardial cells. This is the first report of a myocardial cell lineage for cardiac neural crest cells.

Looping Does Not Occur in a Subpopulation of Zebrafish Embryos After Cardiac Neural Crest Ablation

Premigratory neural crest cells from regions II and III (cardiac) or IV (noncardiac) were ablated at the three to four somite stage by using laser irradiation. We found that the laser was more effective if the embryos were lightly stained with neutral red, a vital dye, before irradiation. The embryos were viable after this ablation, and they could be recognized by a slight depression on the dorsal axis in profile. Notably, all of the embryos with region II/III ablation showed grossly visible signs of cardiac dysfunction after the heart started to beat. Embryos with region IV ablation showed no signs of cardiac dysfunction. AP2 was used as a marker of premigratory neural crest cells. In situ hybridization with AP2 showed a gap in the AP2-expressing neural crest cells consistent with the length of the ablated dorsal neural

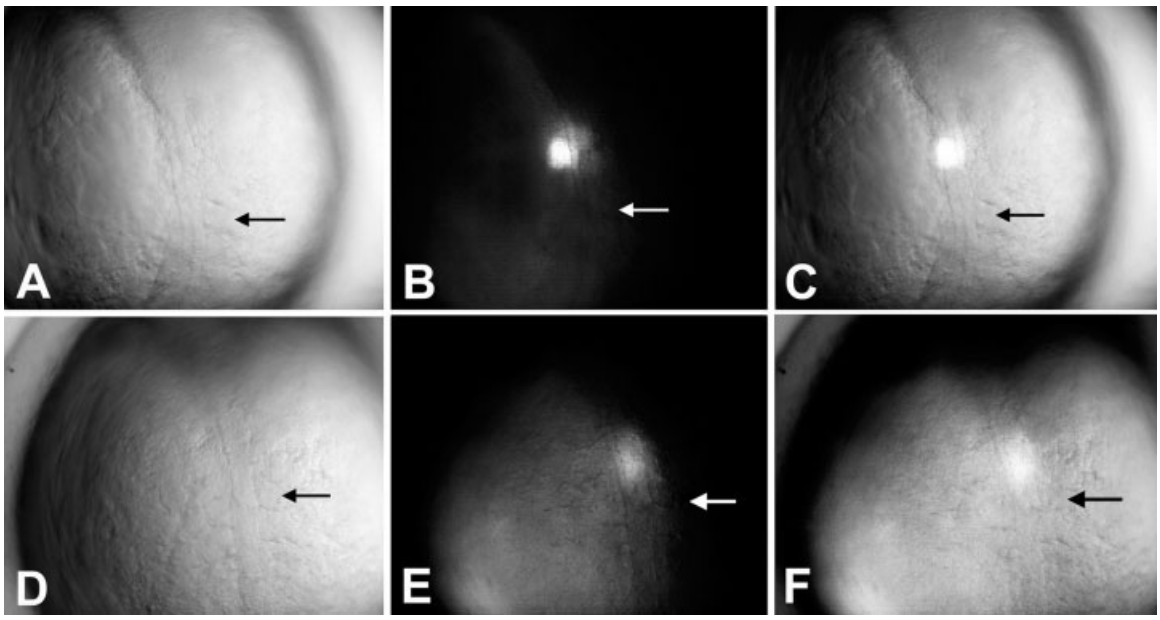

Fig. 2. Two three-somite embryos shown within a few minutes after uncaging fluorescein in the premigratory neural crest. The embryo shown in **A–C** has fluorescein uncaged in region II, and the embryo shown in **D–F** has fluorescein uncaged in area III. In both embryos, the first somite is indicated by the arrows. A and D show brightfield images, B and E are dark field images showing the region uncaged, and C and F show superimposed images.

tube (Table 1B; Fig. 6). HNK1 immunostaining marks migrating neural crest cells in chick and was used for the same purpose in zebrafish. HNK1-expressing cells were absent from the cardiac neural crest migratory pathways after the ablation (Table 1B; Fig. 7).

Videocinephotography of the zebrafish heart was done at 48 hpf as the embryos were lying with their right sides up. This strategy allowed visualization in real time of the myocardial wall and gross features of the heart chambers. The ventricle and conotruncal regions were clearly visible in the sham-operated hearts and showed smooth peristaloid contraction of the atrium followed by the ventricle and conotruncus (online data supplement). Most of the region II/III-ablated zebrafish embryos showed a similar phenotype. However, of the 63 embryos analyzed for gross phenotype after the region II/III neural crest ablation, 13 (20.6%) showed a failure of looping (Table 1B; Fig. 8). In these embryos, the sinus venosus and atrium were clearly visible along with the ventricle and conotruncus, indicating that the hearts did not loop (Fig. 8 and online data supplement). In addition to the lack of apparent looping after cardiac neural crest ablation, the pericardial sac was dilated in these embryos (Fig. 9). Hearts from embryos with region IV ablation appeared normally looped and showed no sign of pericardial dilation.

Cardiac Neural Crest Ablation Causes Decreased Ventricular Function in Zebrafish Embryos

Heart rate in the total group of cardiac neural crest–ablated embryos was significantly depressed (187 bpm, 39 embryos) compared with sham-operated embryos (200 bpm, 43 embryos; $P = 0.024531$). However, heart rate in a subpopulation of neural crest–ablated embryos fell two standard deviations below the mean (Table 3). When this group was removed into its own subgroup, the majority (80%) of the ablated embryos showed heart rates equivalent with sham-operated embryos (200 bpm vs. 200 bpm, $P = 0.6$). The group in which the heart did not loop had significantly depressed heart rates (138 bpm vs. 200 bpm, $P = 7 \times 10^{-14}$). To ensure that the depressed heart rate was not associated with impending mortality, the neural crest-ablated embryos with abnormally low heart rate were isolated and observed over the next 2 days. None of the embryos died in this period, indicating that the decreased heart rate was not associated with embryonic lethality.

Because of the confounding influence of heart rate on functional parameters, ventricular function was determined only in the population of neural crest-ablated embryos that had heart rates equivalent to sham-operated embryos. The most sensitive indicator of decreased contractility is ejection fraction. The ejection fraction in sham-operated embryos was 64% (Table 3). After neural crest ablation the ejection fraction was 53%, a significant decrease ($P < 0.001$). Shortening fraction and stroke volume were also significantly lower in the neural crest-ablated embryos ($P < 0.001$). Cardiac output in sham-operated embryos was approximately 0.06 mm^2/min, and this was depressed by approximately 20% in embryos with neural crest ablations ($P < 0.001$).

DISCUSSION

Our results indicate some surprising differences about the zebrafish cardiac neural crest cell populations

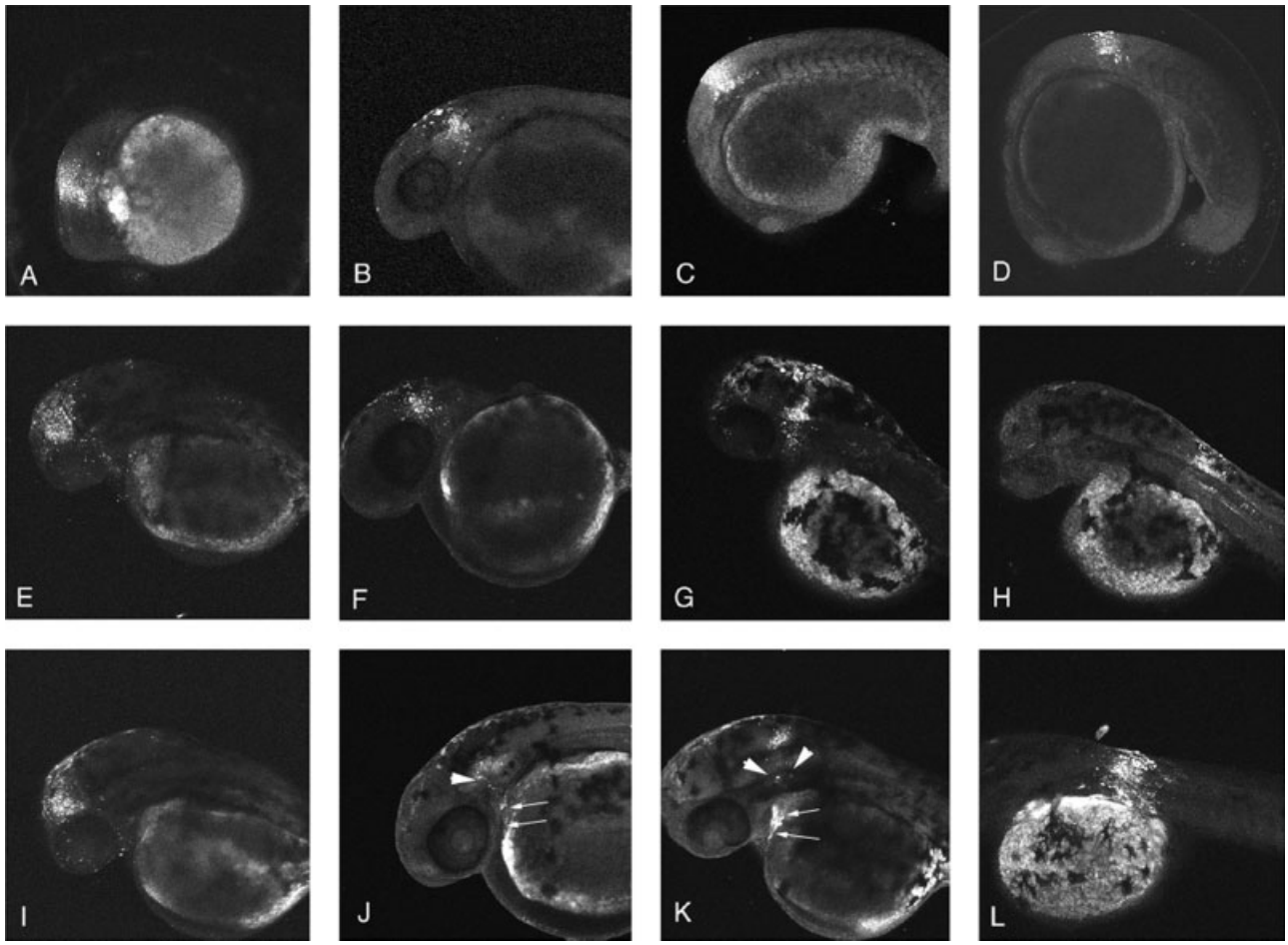

Fig. 3. A series of embryos illustrating the results of uncaging fluorescein in the four different regions of the cranial neural tube. **A–D:** The embryos 3 hr after irradiation at 11 hours postfertilization (hpf). **E–H:** The embryos at 36 hpf. **I–L:** The embryos at 48 hpf. A,E,I, region I; B,F,J, region II; C,G,K, region III; D,H,L, region IV. Cells were found in the branchial arches (arrowheads in J and K) and heart (arrows in J and K) after irradiation of regions II and III.

compared with the chick and mouse. In the zebrafish, the cells originate more rostrally from the neural axis, i.e., above the first somite, than the cardiac neural crest in either mouse or chick, the only two species in which cell fate mapping has been done extensively (Kirby et al., 1983; Fukiishi and Morriss-Kay, 1992). In the zebrafish embryo, the cardiac neural crest cells migrate into and intermingle with the myocardium, adopting a myocardial cell lineage. In contrast, in the chick and mouse, the cardiac neural crest cells in the outflow tract are either mesenchymal and are confined to the cardiac cushions or they form the parasympathetic cardiac ganglia (Waldo et al., 1998, 1999; Kirby and Stewart, 1983). In the zebrafish, the extensive contribution of myocardial cells to the heart by cardiac neural crest cells may explain why ventricular function after cardiac neural crest ablation is worse than that in the chick where cardiac neural crest cells do not contribute to the myocardium (Leatherbury et al., 1990; Tomita et al., 1991). The absence of parasympathetic innervation could also influence heart rate; however, because parasympathetic stimulation causes a negative chronotropic response in most of the vertebrates that have been studied, the heart rate would be expected to be higher in its absence. As little is known about the functional or morphologic innervation of the fish heart, this remains a viable alternative until further work is done.

In avians and mammals, cells derived from the cardiac neural crest provide mesenchymal cells needed for septation of the outflow tract (Kirby et al., 1983). The zebrafish does not have divided systemic and pulmonary circulations; thus, cardiac neural crest cells are not needed to effect septation of the outflow tract. It would be interesting to learn whether the evolutionary need for a divided circulation diverted cardiac neural crest cell subpopulations from a myocardial to a mesenchymal phenotype.

In chick, cardiac neural crest cells also play a role in myocardial maturation by regulating the availability of growth factors in the pharyngeal region (Farrell et al., 2001). In the absence of cardiac neural crest, ventricular function is depressed long before the time neural crest cells normally migrate into the heart (Leatherbury et al., 1990; Tomita et al., 1991). The primary functional deficit is a decrease

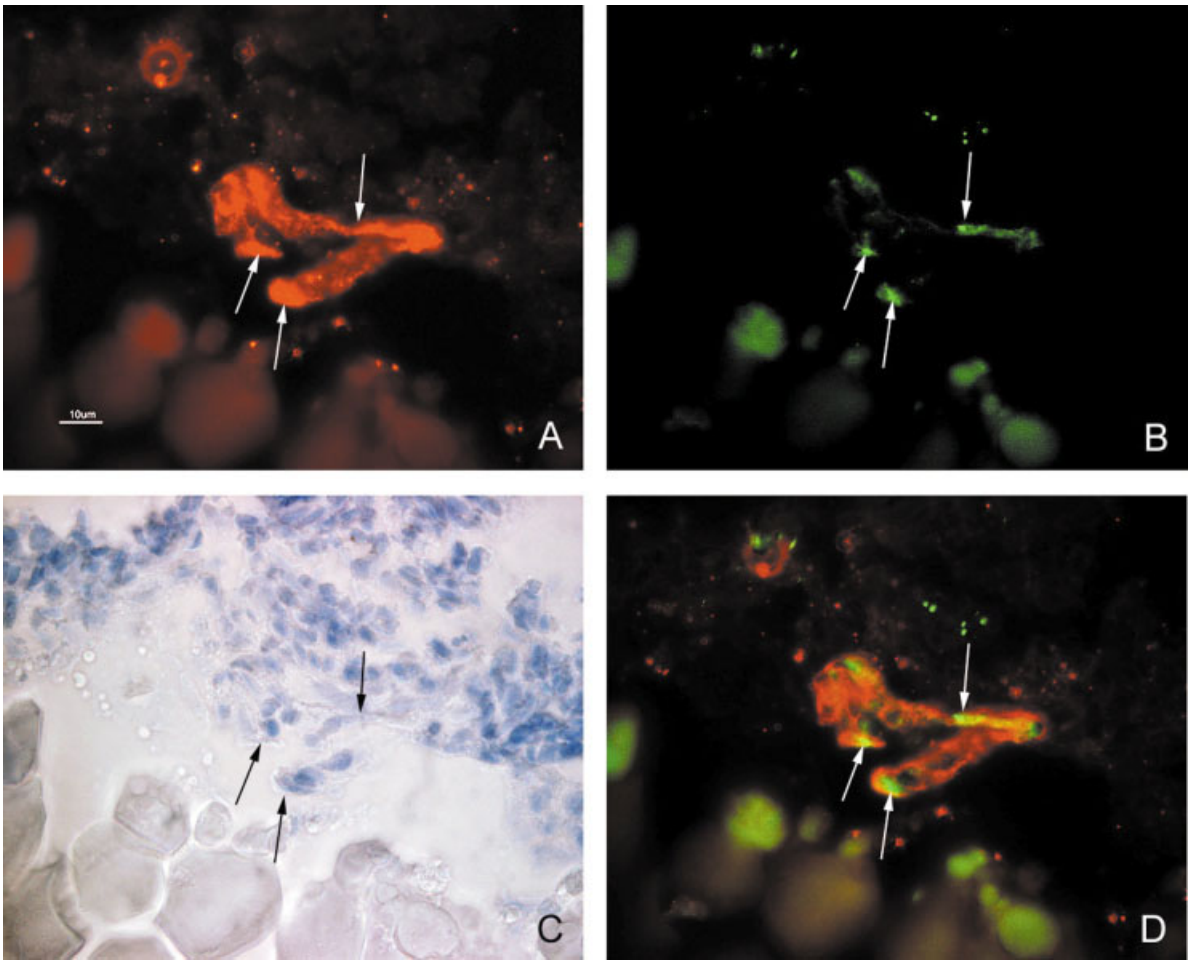

Fig. 4. Unstained frozen sections of two 36 hours postfertilization zebrafish embryos with fluorescein uncaged in region IIBC. **A:** Darkfield image with a rhodamine filter, showing MF20 immunostaining of the outflow tract. **B:** Darkfield image of the same section with a fluorescein filter, showing fluorescein-positive neural crest cells after uncaging in the premigratory neural crest. **C:** Brightfield image stained with thionin. **D:** Darkfield images in A and B have been overlaid to show the colocalization of neural crest cells with MF20 immunoreactivity. The arrows indicate the same three neural crest cells in each panel that express a myocardial phenotype.

in ejection fraction. However, the myocardium also shows decreased calcium transients and L-type calcium current (Farrell et al., 2001; Creazzo et al., 1998). Because these alterations are due to altered signaling in the pharynx, the alteration of myocardial function is an indirect effect.

In contrast, ablation of cardiac neural crest in the zebrafish alters the composition of the myocardial wall by decreasing the number of cardiomyocytes available. There are several differences in the ventricular functional abnormalities between chick and zebrafish with the zebrafish being more severely affected. After neural crest ablation in the zebrafish, both the stroke volume and cardiac output are depressed in addition to depression of the ejection fraction. In neural crest-ablated chick embryos, neither the stroke volume nor the cardiac output is decreased because the heart compensates for decreased stroke volume by ventricular dilation (Leatherbury et al., 1990; Tomita et al., 1991). Because the zebrafish embryo relies on cardiac neural crest for cardiomyocytes, ablation of the cardiac neural crest may decrease the number of cardiomyocytes available for compensation by ventricular dilation. It is possible that the paucity of cardiomyocytes as a consequence of neural crest ablation leads to an inability of the heart to complete the normal looping process that we observed. Although the impetus for looping has been shown in several experimental paradigms to be independent of function, it seems reasonable to assume that the myocyte population might need to be supplemented for looping to occur, especially when the myocardial wall is only one to two cells thick when looping begins (Kousik et al., 2001). Although the looping and heart rate data are reported for different populations of embryos, we observed depressed heart rates in embryos that failed to undergo heart looping.

Our functional measurements were made at 48 hpf when the heart consists of a smooth-walled tube partitioned into four segments identifiable by external constrictions between the segments. The myocardium is one cell thick except for the ventricle, which has two to three cell layers (Hu et al., 2000). At 4 weeks postfertilization,

the outflow tract, which is initially invested in myocardium, shows a smooth muscle wall (Hu et al., 2000). The transition of myocardium to smooth muscle in the outflow tract is in response to the back pressure generated by high resistance in the gills. The outflow tract then functions as a booster pump for the ventricle to maintain a steady blood flow into the gills (Icardo et al., 1999a,b). Of interest, cardiac neural crest cells in the chick provide the smooth muscle in the tunica media of the great arteries; however, they appear to adopt a fibroblast cell lineage in the outflow tract septum (Waldo et al., 1998).

The cardiac outflow tract is a complex structure that, in avians and mammals with divided systemic and pulmonary circulations, is dependent

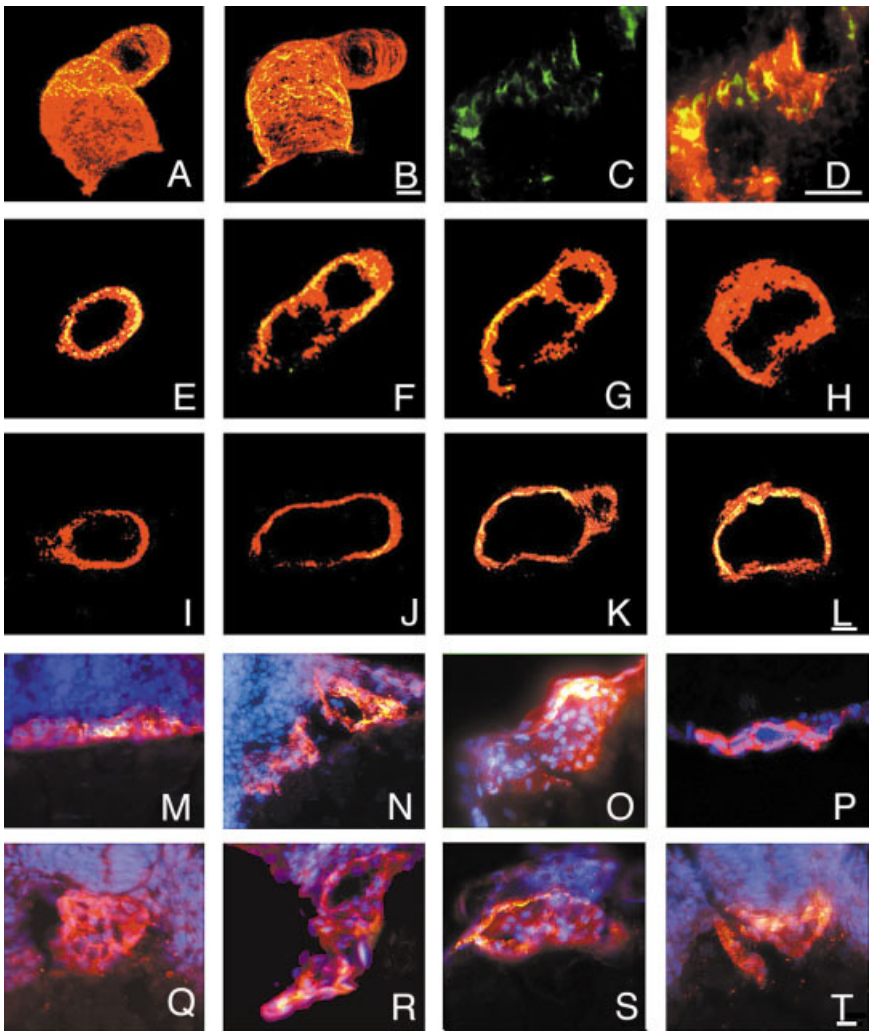

Fig. 5. Neural crest cells were uncaged in regions II and III for identification of the proportion of myocardial cells derived from cardiac neural crest. The embryos have been triple stained with antifluorescein (green), MF20 (red) and DAPI (blue). **A** and **B**: Reconstruction of 30 layers visualized by laser confocal microscopy 36 hr after dye was uncaged in region II and region III, respectively. The neural crest-derived myocardial cells from region II are most densely localized to the outflow and ventricle. The neural crest-derived myocardial cells from region III are most densely localized to the inflow and atrium. C and D are frozen sections of the outflow region from hearts in embryos with dye uncaged in region II showing dense contribution of neural crest cells to the myocardium. **C**: Uncaged dye showing the localization of neural crest cells. **D**: C is superimposed on the MF20 stained image to show colocalization of neural crest cells and MF20 (yellow). E-H and I-L are single layers from A and B, respectively, showing the localization of neural crest cells from region II and region III in the various parts of the heart. Yellow shows colocalization of MF20 and neural crest cells. **E** and **I**: outflow, **F** and **J**: outflow and ventricle, **G** and **K**: ventricle and atrium, **H** and **L**: inflow. M-P and Q-T show frozen sections of the hearts with dye uncaged in regions II and III, respectively. **M** and **Q**: outflow, **N** and **R**: ventricle and atrium, **O** and **S**: atrium, **P** and **T**: inflow. All bars are 20 um.

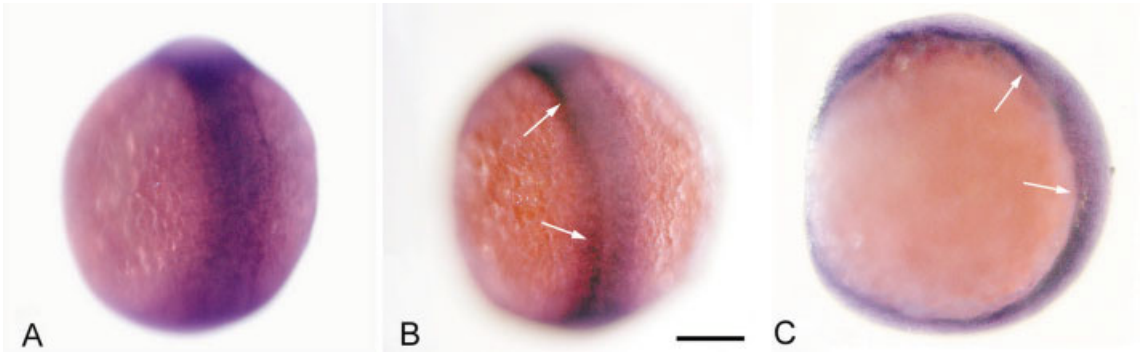

Fig. 6. Sham-operated (**A**) and cardiac neural crest-ablated (**B,C**) embryos (eight somites) 3 hr after the ablation procedure and AP2 whole-mount in situ hybridization demonstrate the extent of the premigratory neural crest that is missing. A and B show dorsal views and C is a sagittal view. The head is up in each panel. White arrows indicate the region of neural crest that is missing. Scale bar = 100 μ.

TABLE 2. Percentage of CNC-Derived Myocardial Cells From Regions II and III in Various Segments of the Heart[a]

Heart region myocardial cells	Outflow		Ventricle		Atrium		Inflow	
	CNC	Total	CNC	Total	CNC	Total	CNC	Total
Region II	12.2 ± 3.0	52.0 ± 16.2	12.2 ± 3.3	67.2 ± 21.6	3.4 ± 1.1	65.0 ± 2.2	0.4 ± 0.6	19 ± 5.0
%		23.4		18.2		5.2		2.1
Region III	0.8 ± 0.8	53.0 ± 43.7	5 ± 1.9	59.2 ± 18.4	13.0 ± 2.4	51.6 ± 8.0	7.8 ± 2.7	66.4 ± 18.4
%		1.5		8.5		25.2		11.8

[a]Data represents mean ± SD. n = 5 for each region. CNC, cardiac neural crest.

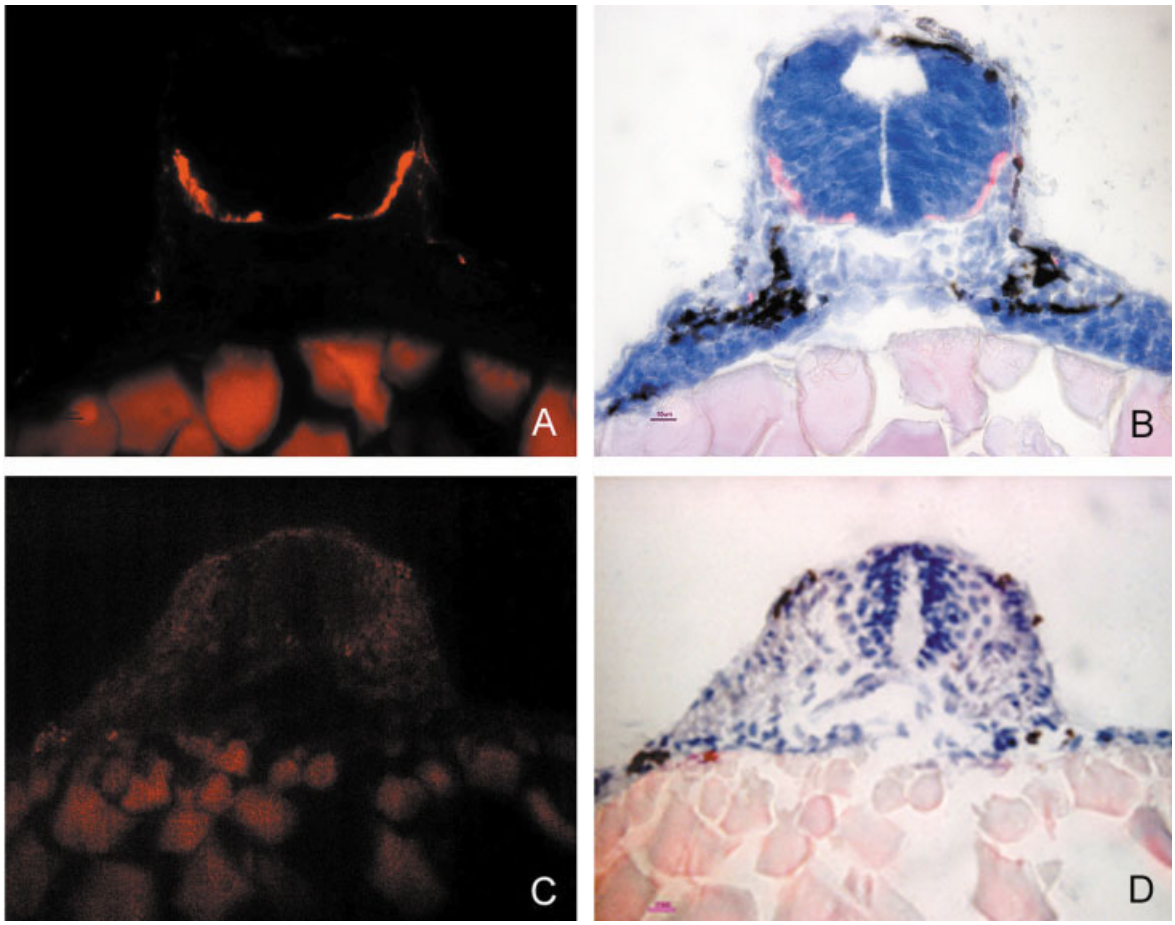

Fig. 7. Neural crest cells can be identified by HNK1-positive staining (arrows) in sham-operated embryos (**A,B**) but are not seen in cardiac neural crest–ablated embryos (**C,D**). The cardiac neural crest arising from regions II and III was ablated in the embryo shown in C and D. This resulted in a dramatically reduced population of HNK1-positive cells migrating around the neural tube in 24 hours postfertilization embryos.

on extracardiac mesenchyme provided by the cardiac neural crest for normal development. This part of the heart, i.e., the conotruncus, is particularly prone to congenital malformation in human development. Understanding the role and evolutionary history of cardiac neural crest cells in a vertebrate with an undivided cardiac outflow provides new insight into the complex interactions of the various cell types that make up the divided outflow tract. The cardiac dysfunction associated with abnormal heart development leads to a high incidence of prenatal lethality and is frequently life-threatening for newborns. In understanding the impact of cardiac neural crest cells on myocardial development, we will have a better opportunity for preventing the dysfunction associated with heart defects and attenuating the consequences of cardiac dysmorphogenesis.

EXPERIMENTAL PROCEDURES

Zebrafish Maintenance

Adult zebrafish were maintained and bred, and embryos were raised as described by Westerfield (1995).

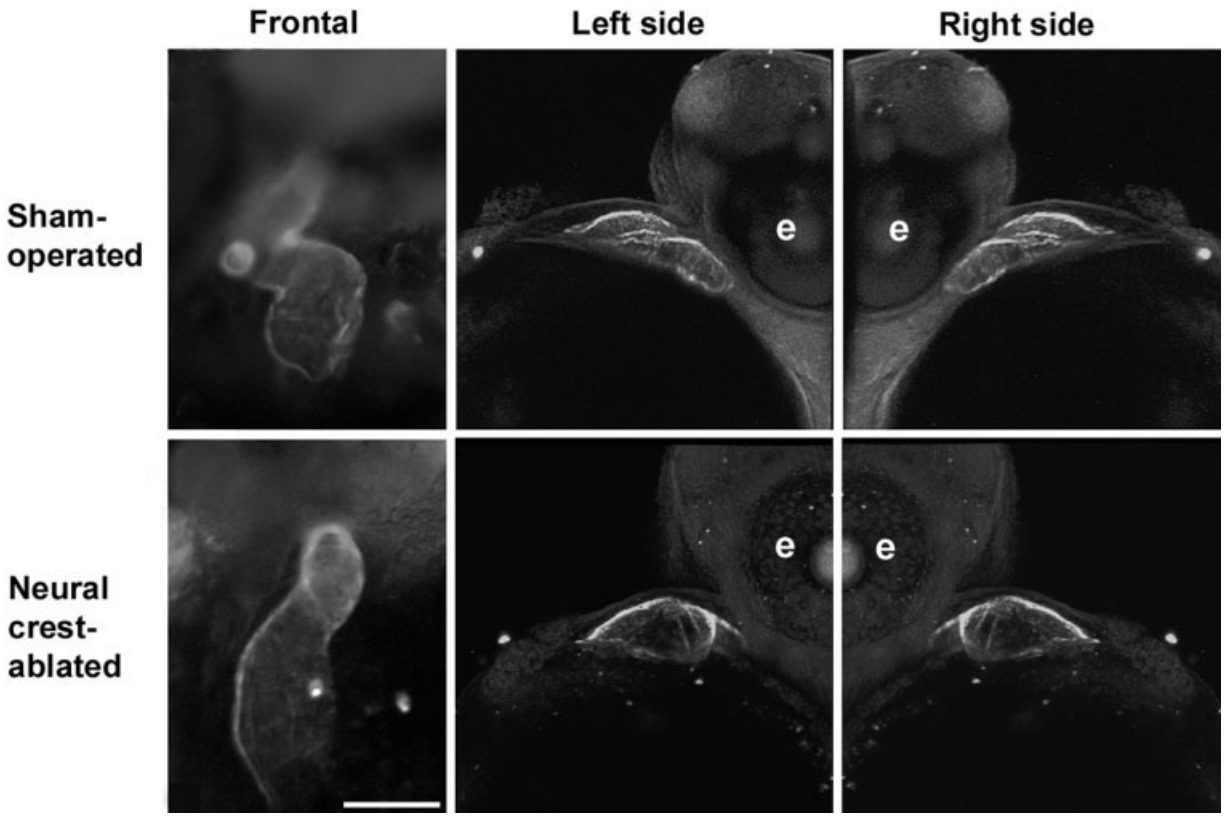

Fig. 8. Cardiac neural crest ablation causes failure of looping in a subset of embryos. Sham-operated and neural crest-ablated embryos (48 hours postfertilization) shown in whole-mount after MF20 staining. The embryos shown in a frontal view are different from those shown from the right and left sides, which were viewed by confocal microscopy. Movies of the embryos shown from the side are available in the online data supplement. The atrial and ventricular chambers are superimposed in the sham-operated embryos in both views, whereas the chambers are not superimposed in the ablated embryos.

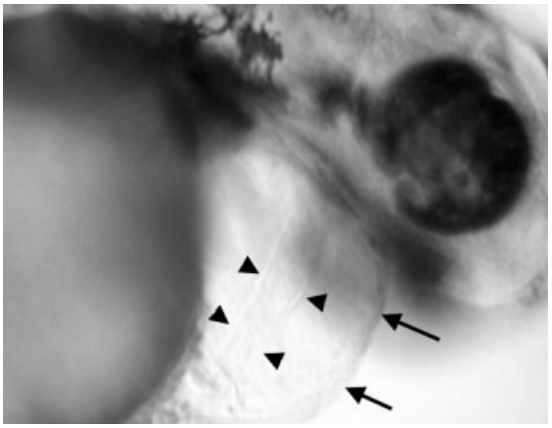

Fig. 9. Neural crest–ablated embryo at 48 hours postfertilization viewed from the right side, showing the enlarged space between the heart tube and the pericardium, which is indicative of pericardial effusion. The arrowheads delineate the heart tube, whereas the arrows show the pericardium.

Cell Tracing by Photoactivatable Probe

Cell lineage experiments in zebrafish embryos are possible by using laser irradiation to uncage fluorescein from DNMB-caged fluorescein dextran (Stainier and Fishman, 1993, 1994). Zebrafish embryos at the one- to two-cell stage were injected with a 0.25% solution of DMNB-caged fluorescein dextran (Molecular Probes) in 0.1 M KCl (modified from Serbedzija et al., 1998). The injected embryos were maintained at 28.5°C until the desired stage is reached. At the three- to four-somite stage, they were placed in an agar ramp and positioned such that the somites and dorsal midline could be visualized. The caged dye was activated by exposing small patches of cells to 50 pulses of laser light (laser dye was Coumarin 480 with a peak of 470, Laser Science, Inc.) generated by a nitrogen pulsed laser focused through a 40× objective on an Olympus stereomicroscope. Activation of the dye was confirmed by visual examination 3 hr after uncaging. The embryos were maintained at 28.5°C.

Confocal laser scanning microscopy was used to collect images from live zebrafish embryos at 36 to 48 hr after the dye uncaging. Embryos were removed from their cho-

rions manually or by using pronase (0.2 mg/ml for 5 min), anesthetized with Tricaine, and positioned on a coverslip. To observe the uncaged DMNB-fluorescein dextran in cells, a 488-nm filter was used on a Bio-Rad MRC-1024UV system. Whole-mount embryos were viewed at ×40 and ×60 magnification. Fifteen to 20 images were collected in 0.5-μm-thick steps for each embryo. The images were stacked to yield a single image.

TABLE 3. Ventricular Contractility in Sham-operated and Neural Crest-ablated Zebrafish Embryos at 48 hpf

Parameter	Sham-operated	Neural crest-ablated	p
N	43	45	
Shortening fraction (%)	30.19 ± 1	25.45 ± 1	<0.001
Ejection fraction (%)	64.66 ± 1.2	53.81 ± 1.2	<0.001
Stroke volume (mm^2)	0.0003 ± 1.26E-05	0.00024 ± 1.00E-05	<0.001
Heart rate (beats/min)	200 ± 4	189 ± 3	>0.05
Cardiac output (mm^3/min)	0.06 ± 0.003	0.05 ± 0.002	>0.001

AP2 In Situ Hybridization

AP2 is a gene expressed in premigratory neural crest. Two specific fragments of zebrafish AP2 cDNA were cloned to generate in situ hybridization probes: AP2a is a 297-bp fragment located between 962 and 1258. The PCR primers areas follows: forward primer 5′-GACTGAGTTTCCAGCCAAGG and reverse primer 5′-GCTTTAATTGCCTCCGTCAG. AP2b is a 351-bp fragment located between positions 2046 to 2397 cloned by forward primer 5′-GCGACACTGAAGCAAGTGAA and reverse primer 5′-AGCTATTGCCAGCACAGGTT.

Neural Crest Ablation

For the ablations, three- to four-somite stage embryos were lightly stained with neutral red. A pulsed nitrogen/dye laser (VSL-377/DLM-110; Laser Science, Inc., Newton, MA) was used to ablate the dorsal midline where premigratory neural crest cells originate. The dye used in the laser was Coumarin 440 (peak: 445 nm), and the laser was set for 10–15 pulses/sec. Sham-operated embryos were prepared simultaneously by staining with neutral red. The quality of the surgery was monitored by using the neural crest marker antibody HNK-1 in 24-hr embryos.

Immunohistochemistry

After visualization by confocal microscopy as whole-mounts, the embryos were frozen in liquid nitrogen-cooled isopentane, mounted with OCT, and sectioned in a cryostat at 12 microns. The sections were stained with MF20, a monoclonal antibody for myosin heavy chain. MF20 was used undiluted for 1 hr at room temperature, followed by 30 min in secondary antibody diluted 1:1,000 (ABC peroxidase mouse kit, Vector Laboratories, Burlingame, CA). All sections were visualized with diaminobenzidine (Vector) for 10 min and lightly counterstained with hematoxylin (diluted 1:10 in 1% glacial acetic acid). The MF20 was obtained from the Developmental Studies Hybridoma Bank under the auspices of the NICHD and maintained by The University of Iowa, Department of Biological Sciences (Iowa City IA).

For HNK1 (Developmental Studies Hybridoma Bank) immunohistochemistry, the zebrafish embryos were fixed overnight at 4°C in 0.4% paraformaldehyde pH 7.2 with 0.1 M sodium phosphate buffer containing 0.025% $CaCl_2$ and 3% sucrose. The embryos were washed three times with phosphate buffered saline (PBS) for 5 min and then placed in distilled water for 10 min, after which they were dehydrated in methanol and stored at −20°C overnight. The embryos were rehydrated through graded methanols in PBS and placed in blocking solution at room temperature for 1 hr (5% sheep serum, 1% bovine serum albumin (BSA), 1% dimethyl sulfoxide, 0.1% Tween20 in PBS). Primary staining was done with HNK1 supernatant at 4°C overnight. The embryos were extensively washed with 1% BSA in PBST and incubated at 4°C overnight with gentle rocking in Alexa Fluor 568 goat anti-mouse immunoglobulin G (H+L), 2 mg/ml diluted 1:50 in blocking solution. The embryos were washed extensively in 1% BSA in PBST and finally in PBS.

Analysis of Heart Function

Heart rate was determined in 34 neural crest–ablated embryos and 24 sham-operated embryos at 48 hpf. Beats per minute were calculated from 20 sec of counting. Heart function was assessed essentially the same as has been reported previously by our group for chick embryos with some modification in the visual assessment for collecting digitized areas based on the difference in shape of chick and zebrafish ventricles (Leatherbury et al., 1990). At 48 hpf, the embryos were filmed with a Kodak Ektapro Imager 1000HRC using a stereomicroscope (Olympus, SZH10, C-squared Corp, Marietta, GA). The embryos were held in a waterbath at 28.5°C until the time of filming. They were then removed one at a time, placed in a small culture dish, and filmed for 5 sec at 250 frames/sec at a magnification factor of × 140. The temperature was monitored during filming by using a thermister probe placed adjacent to the embryo. A scribed glass standard was also filmed to allow exact calibration of the magnification factor. The films were later uploaded to a high-resolution 13-inch monitor, and four frames of diastole and three of systole were chosen for

each embryo. End-diastolic and end-systolic frames were chosen and analyzed with VISILOG software (version 4.1, Noesis Vision, Inc., Quebec, Canada).

ACKNOWLEDGMENTS

We thank Mary Redmond Hutson for discussion and suggestions during the course of these experiments, Michael Farrell for comments on the manuscript, and Ping Zhang for help with the AP2 in situ hybridization.

REFERENCES

Bockman DE, Kirby ML. 1984. Dependence of thymus development on derivatives of the neural crest. Science 223:498–500.

Bockman DE, Redmond ME, Waldo K, Davis H, Kirby ML. 1987. Effect of neural crest ablation on development of the heart and arch arteries in the chick. Am J Anat 180:332–341.

Bockman DE, Redmond ME, Kirby ML. 1989. Alteration of early vascular development after ablation of cranial neural crest. Anat Rec 225:209–217.

Conway SJ, Godt RE, Hatcher CJ, Leatherbury L, Zolotouchnikov VV, Brotto MA, Copp AJ, Kirby ML, Creazzo TL. 1997. Neural crest is involved in development of abnormal myocardial function. J Mol Cell Cardiol 29:2675–2685.

Creazzo TL. 1990. Reduced ``L'' type calcium current in the embryonic chick heart with persistent truncus arteriosus. Circ Res 66:1491–1498.

Creazzo TL, Brotto MA, Burch J. 1997. Excitation-contraction coupling in the day 15 embryonic chick heart with persistent truncus arteriosus. Pediatr Res 42(6):731–737.

Creazzo TL, Godt RE, Leatherbury L, Conway SJ, Kirby ML. 1998. Role of cardiac neural crest cells in cardiovascular development. Ann Rev Physiol 60:267–286.

Farrell MJ, Burch JL, Kumiski DH, Stadt HA, Godt RE, Creazzo TL, Kirby ML. 2001. FGF-8 suppresses development of myocardial calcium transients after neural crest ablation. J Clin Invest 107: 1509–1517.

Fishman MC, Chien KR. 1997. Fashioning the vertebrate heart: earliest embryonic decisions. Development 124:2099–2117.

Fukiishi Y, Morriss-Kay GM. 1992. Migration of cranial neural crest cells to the pharyngeal arches and heart in rat embryos. Cell Tissue Res 268:1–8.

Goodrich ES. 1958. Studies on the structure and development of vertebrates. Vol 2. New York: Dover Publ., Inc.

Hu N, Sedmera D, Yost HJ, Clark EB. 2000. Structure and function of the developing zebrafish heart. Anat Rec 260:148–157.

Icardo JM, Colvee E, Cerra MC, Tota B. 1999a. Bulbus arteriosus of the Antarctic teleosts. II. The red-blooded Trematomus bernacchii. Anat Rec 256:116–126.

Icardo JM, Colvee E, Cerra MC, Tota B. 1999b. Bulbus arteriosus of the Antarctic teleosts. I. The white-blooded Chionodraco hamatus. Anat Rec 254: 396–407.

Kimmel CB, Ballard WW, Kimmel SR, Ullmann B, Schilling TF. 1995. Stages of embryonic development of the zebrafish. Dev Dyn 203:253–310.

Kirby ML, Stewart DE. 1983. Neural crest origin of cardiac ganglion cells in the chick embryo: identification and extirpation. Dev Biol 97:433–443.

Kirby ML, Gale TF, Stewart DE. 1983. Neural crest cells contribute to aorticopulmonary septation. Science 220:1059–1061.

Kirby ML, Creazzo TL. 1995. Cardiovascular development. Neural crest and new perspectives. Cardiol Rev 3:226–235.

Koushik SV, Wang J, Rogers R, Moskophidis D, Lambert NA, Creazzo TL, Conway SJ. 2001. Targeted inactivation of the sodium-calcium exchanger (Ncx1) results in the lack of a heartbeat and abnormal myofibrillar organization. FASEB J. 15:1209–1211.

Leatherbury L, Gauldin HE, Waldo KL, Kirby ML. 1990. Microcinephotography of the developing heart in neural crest-ablated chick embryos. Circulation 81: 1047–1057.

Leatherbury L, Connuck DM, Gauldin HE, Kirby ML. 1991. Hemodynamic changes and compensatory mechanisms during early cardiogenesis after neural crest ablation in chick embryos. Pediatr. Res 30:509–512.

Schilling TF, Kimmel CB. 1994. Segment and cell type lineage restrictions during pharyngeal arch development in the zebrafish embryo. Development 120:483–494.

Serbedzija GN, Chen JN, Fishman MC. 1998. Regulation in the heart field of zebrafish. Development 125:1095–1101.

Stainier DYR, Fishman MC. 1993. Cardiovascular development in the zebrafish. I. Myocardial fate map and heart tube formation. Development 119:31–40.

Stainier DYR, Fishman MC. 1994. The zebrafish as a model system to study cardiovascular development. Trends Cardiovasc Med 4:207–212.

Terada N, Hamazaki T, Oka M, Hoki M, Mastalerz DM, Nakano Y, Meyer EM, Morel L, Petersen BE, Scott EW. 2002. Bone marrow cells adopt the phenotype of other cells by spontaneous cell fusion. Nature 416:542–545.

Tomita H, Connuck DM, Leatherbury L, Kirby ML. 1991. Relation of early hemodynamic changes to final cardiac phenotype and survival after neural crest ablation in chick embryos. Circulation 84:1289–1295.

Waldo KL, Willner W. Kirby ML. 1990. Origin of the proximal coronary artery stem and a review of ventricular vascularization in the chick embryo. Am J Anat 188:109–120.

Waldo KL, Kumiski D, Kirby ML. 1996. Cardiac neural crest is essential for the persistence rather than the formation of an arch artery. Dev Dyn 205:281–292.

Waldo KL, Miyagawa-Tomita S, Kumiski D, Kirby ML. 1998. Cardiac neural crest cells provide new insight into septation of the outflow tract: Aortic sac to ventricular septal closure. Dev Biol 196: 129–144.